JOURNAL OF VIROLOGY, Mar. 2008, p. 2456–2469 Vol. 82, No. 5
0022-538X/08/$08.00+0 doi:10.1128/JVI.01665-07

The Programmed Death-1 and Interleukin-10 Pathways Play a Down-Modulatory Role in LP-BM5 Retrovirus-Induced Murine Immunodeficiency Syndrome▽

Kathy A. Green,[1] Taku Okazaki,[2] Tasuku Honjo,[2] W. James Cook,[1]† and William R. Green[1]*

Department of Microbiology and Immunology, Dartmouth Medical School, and Norris Cotton Cancer Center, Lebanon, New Hampshire 03756,[1] and Department of Immunology and Genomic Medicine, Graduate School of Medicine, Kyoto University, Yoshida-Konoe, Sakyo-ku, Kyoto 606-8501, Japan[2]

Received 31 July 2007/Accepted 11 December 2007

Pathology due to the immune system's response to viral infections often represents a delicate balance between inhibition of viral pathogenesis and regulation of protective immunity. In susceptible C57BL/6 (B6) mice, the murine retroviral isolate LP-BM5 induces splenomegaly, hypergammaglobulinemia, profound B- and T-cell immunodeficiency, and increased susceptibility to opportunistic pathogens and terminal B-cell lymphomas. Here, we report that B6.PD-1 (programmed death-1) and B6.IL-10 knockout mice are substantially more susceptible to LP-BM5-induced disease than wild-type B6 mice. LP-BM5-infected B6.PD-1$^{-/-}$ mice developed more severe splenomegaly, hypergammaglobulinemia, and immunodeficiency than infected B6 mice: PD-1$^{-/-}$ mice are more susceptible to lower doses of LP-BM5 and show more exaggerated disease early postinfection. LP-BM5-infected B6.IL-10$^{-/-}$ mice also develop exaggerated LP-BM5-induced disease, compared to B6 mice, without a significant change in the retroviral load. By reciprocal reconstitution experiments, comparing wild-type versus PD-1$^{-/-}$ sources of the requisite cells for LP-BM5 pathogenesis—CD4 T and B cells, PD-1^{+} B cells appear to be crucial in the normal limitation of LP-BM5-induced disease in B6 mice. Also, infected B6 mice have increased CD11b^{+} spleen cells that express interleukin-10 (IL-10). However, PD-1$^{-/-}$ mice, though showing an even greater expansion of CD11b^{+} cells after LP-BM5 inoculation, did not show an equivalent increase in IL-10-producing cells. Thus, it appears that PD-1/PD-L interactions and IL-10 are primarily important in moderating the effects of LP-BM5-induced disease in B6 mice.

While neutralizing antibody responses are often critical upon virus reinfection, or in response to an initial virus challenge following analogous vaccination, cell-mediated immunity also frequently plays an important role in protection. CD8^{+} T-cell effector responses in particular, but also CD4^{+} T cells that mediate T-cell help and/or serve as effectors themselves, can be crucially important in protecting against, or limiting the extent of, viral infections. Cell-mediated immunity is especially relevant during the time span before high-titer, high-affinity neutralizing antibody responses may be generated. Recently, it has become apparent during several chronic viral infections, including human immunodeficiency virus (HIV)/AIDS, that normal immune down-regulating mechanisms, such as the programmed death-1 (PD-1) pathway, may be a crucial factor in limiting the magnitude or duration of antiviral T-cell responses, such that virus is not cleared or controlled. Strategies to inhibit such negative regulation, and thereby improve protective T-cell immunity, are therefore attractive. However, responses by T cells can also be responsible for the immunopathology observed in many disease states, including viral infections. Thus, an understudied possibility is that interventions to abrogate or diminish negative regulation by inhibitory molecules such as PD-1 may unwittingly augment not only protective antiviral T-cell immunity but also T-cell responses that contribute to pathogenesis.

After infection with the LP-BM5 murine leukemia retrovirus isolate, a disease syndrome which includes profound immunodeficiency develops in certain inbred strains of mice such as the highly susceptible C57BL/6 (B6) strain (3, 11, 26, 28, 47). By about 3 weeks postinfection (wpi) with LP-BM5, activation-related events, which include hypergammaglobulinemia (hyper-Ig) and splenomegaly, become easily detectable in LP-BM5-infected B6 mice. Beginning at approximately 6 wpi, a profound immunodeficiency is readily apparent, including severely dampened T- and B-cell responses, leading to the full array of disease features (8, 10, 33, 34, 40, 46, 48, 54, 66). Thus, there is an increased susceptibility to disease progression and death when mice are exposed to environmental pathogens that normally cause limited infections, and at later time points LP-BM5-infected B6 mice develop B-cell lymphomas. Many of the disease features of this murine retrovirus-induced immunodeficiency disease are similar to those that afflict individuals with HIV/AIDS (4, 43, 49).

Inoculation of LP-BM5 into B6 mice genetically deficient in or subjected to prior in vivo depletion of either CD4^{+} T cells or B cells leads to infection but not to virus-induced disease (10, 22, 23, 41, 42, 66, 73). To further characterize the requirement for these lymphoid subsets, we determined that CD154/CD40 interactions are necessary for both the induction and progression of LP-BM5 pathogenesis. In vivo treatment with anti-CD154 (CD40 ligand) monoclonal antibody (MAb) either at the initiation of or 3 to 4

* Corresponding author. Mailing address: Department of Microbiology and Immunology, Dartmouth Medical School, 1 Medical Center Drive, Lebanon, NH 03756. Phone: (603) 650-5056. Fax: (603) 650-6223. E-mail: kathy.a.green@dartmouth.edu.

† Present address: GlycoFi/Merck & Co., Inc., Lebanon, NH 03766.

▽ Published ahead of print on 19 December 2007.

weeks after infection of B6 mice led to substantial inhibition of splenomegaly, hyper-Ig, and B- and T-cell immunodeficiency (21, 22). As confirmation of a requirement for a CD154/CD40 molecular interaction for LP-BM5-induced disease, we and others have reported that, compared to wild-type (WT) B6 mice, B6.CD154 (23) and CD40 (23, 74) knockout (KO) mice are resistant to LP-BM5-induced disease. Further, by reciprocal adoptive-transfer experiments, we directly demonstrated that $CD4^+$ T cells and B cells are necessary, respectively, for the requisite CD154 and CD40 expression in LP-BM5-induced disease (23). Prompted by studies showing that CD154 oligomerization of CD40 results in the recruitment of cytoplasmic TRAF (tumor necrosis factor receptor-associated factor) proteins to the classic shared TRAF2,3/5 versus TRAF6 binding sites of the CD40 cytoplasmic tail domain (37, 56, 57), our laboratory has also reported that LP-BM5-induced disease depends specifically on CD40-TRAF6 signaling (20). However, the paradigm that the functional consequences of ligation of CD40 on B cells, via a number of overlapping signal transduction pathways, often ultimately are dependent on the well-known downstream up-regulation of the costimulatory ligands for CD28 and CTLA-4, i.e., B7-1 (CD80) and B7-2 (CD86) (9, 32, 58, 59, 61), does not appear to explain LP-BM5 disease. Thus, we showed that B6.CD80/CD86 double-KO mice were susceptible to LP-BM5-induced disease (24). Therefore, CD154 ligation of CD40 in LP-BM5-induced disease does not serve simply to accomplish the classic up-regulation of CD80/CD86 but rather may up-regulate the expression of other molecules that may be required for the induction or regulation of virus-induced disease—perhaps other cell surface "costimulatory" molecules and/or cytokines, including down-modulatory cytokines such as IL-10.

Here, based on initial microarray RNA expression profiling, we address the possible role of the PD-1/PD-L1/PD-L2 and IL-10 pathways in LP-BM5-induced disease. PD-1 (CD279), a transmembrane protein belonging to the CD28/CTLA4 subfamily, was originally identified in a T-cell line undergoing apoptotic cell death (30). PD-1 is generally thought to direct inhibitory functions, but unlike that of CTLA-4, with which it shares 23% amino acid homology, PD-1 expression can be induced not only in T cells but also in B cells and certain other cell types (25, 52). The PD-1 molecule contains an extracellular immunoglobulin V (IgV)-like domain and cytoplasmic immunoreceptor tyrosine-based inhibitory motif and immunoreceptor tyrosine-based switch motif domains. Antigen-stimulated expression of PD-1 is followed by recruitment of tyrosine phosphatase src homology 2 domain-containing tyrosine phosphatase 2 to the immunoreceptor tyrosine-based switch motif, but not to the immunoreceptor tyrosine-based inhibitory motif, site (51, 53, 62). Two PD-1 ligands—PD-L1 (CD274) and PD-L2 (CD273)—have been described, and both are type 1 transmembrane proteins containing IgV- and IgC-like domains (18, 39). Both negative and positive effects on T-cell activation have been reported following PD-1 ligation by PD-L1 and PD-L2 (13, 15, 18, 39). PD-L1, constitutively expressed by T and B cells, macrophages, and dendritic cells (DC), is additionally upregulated after activation, unlike PD-L2 expression, which is much less prevalent and present mainly on activated macrophages and DC (15, 72). Both ligands are also found on tumor cells from various tissue and organ sites (13, 16, 67). Although many direct and indirect mechanisms of action have been suggested following PD-1 ligation, of special note to the present investigation, it has been reported that in vitro activation strategies such as anti-CD3 and PD-L1 stimulation result in increased secretion of IL-10 (15, 38, 68). IL-10 has also recently been shown to induce the expression of PD-L1 on monocytes (64, 65) and to be a key player in acute versus chronic lymphocytic choriomeningitis virus (LCMV) infection (7, 17). In general (not relating to primarily IL-10 studies), several reports have detailed the role of the PD-1/PD-L pathway in mouse and human viral diseases such as hepatitis C and HIV-induced AIDS (5, 14, 31, 55, 69, 70).

MATERIALS AND METHODS

Mice. Seven-week-old male B6 mice were purchased from the National Institutes of Health (Bethesda, MD), housed in the Dartmouth Medical School Animal facility, and used when 8 to 10 weeks of age. Breeding pairs fully backcrossed to B6 IL-10 KO mice obtained from The Jackson Laboratory (Bar Harbor, ME) were originally derived as previously described (36). B6-backcrossed PD-1 KO breeding pairs derived as reported previously (50) were obtained from Jian Zhang Rush-Presbyterian-St. Luke's Medical Center, Chicago, IL. B6.Rag-1 KO mice purchased from The Jackson Laboratory were employed as recipients in adoptive-transfer experiments in which equal numbers were reconstituted with purified $CD4^+$ T and B cells from various donor mice.

Splenocyte subpopulation preparation. For cellular reconstitution of Rag-1 KO mice, splenocyte suspensions were labeled with anti-CD19 (1D3)- or anti-CD4 (L3T4)-coupled paramagnetic beads and subjected to column purification according to the manufacturer's (MACS; Miltenyi Biotec, Auburn, CA) protocol. Purified B-cell populations were obtained by incubation with anti-CD19 beads, positively selecting for $CD19^+$ B cells, and subsequently the flowthrough cells were labeled with anti-CD4 beads, positively selecting for $CD4^+$ T cells. These selection approaches yielded cell preparations which were $\geq$98% $B220^+$ or $\geq$90% $CD4^+$ enriched, respectively, as detected by flow cytometric analyses.

LP-BM5 virus inoculations. LP-BM5 was prepared in our laboratory as previously described (33). G6 cells, originally generously provided by Janet Hartley and Herbert Morse (NIH affiliation), a cloned cell line from SC-1 cells infected with the LP-BM5 virus mixture, were used in a coculture with uninfected SC-1 cells to produce LP-BM5 virus stocks. As noted in Results, mice were infected intraperitoneally with 1×10^5, 5×10^4, 2×10^4, or 3×10^2 ecotropic PFU as determined by a standard retroviral XC plaque assay (60).

ELISA determinations of serum immunoglobulins. To measure serum hyper-Ig, capture antibodies, affinity-purified goat anti-mouse IgG2a or IgM (Southern Biotechnology Associates, Birmingham, AL), were used to coat 96-well plates after which enzyme-linked immunosorbent assays (ELISAs) were conducted as previously described (21, 22, 23, 41, 42). The averages of experimental groups were statistically compared by the Student *t* test.

Spleen cell response to mitogens. Spleen cells (4×10^5) from control and experimental mice were plated in triplicate into 96-well plates with medium containing 5% fetal calf serum, L-glutamine, antibiotics, and a final concentration of 2 μg/ml ConA or 10 μg/ml LPS. After 72 h, all wells were pulsed with 1 μCi of [^{3}H]thymidine (Dupont NEN, Boston, MA) and harvested (Packard, Meriden, CT) 6 h later for assessment of thymidine incorporation by scintillation counting (Packard, Meriden, CT). The averages of experimental groups were statistically compared by the Student *t* test.

In vivo MAb blocking. Ascites preparations were obtained for the following MAbs: anti-PD-1 (J43; reference 1), anti-PD-L1 (1 to 111A; reference 29), and anti-PD-L2 (54S; reference 29). A dose of 100 μl was administered intraperitoneally to LP-BM5-infected B6 mice three times a week for either 3 or 7.5 weeks as indicated in Results.

Flow cytometry. For extracellular staining, 5×10^5 spleen cells were incubated with fluorescein isothiocyanate (FITC)-, phycoerythrin-, allophycocyanin (APC)-, or Cy-Chrome-conjugated antibodies, followed by direct immunofluorescence, as quantified by log amplification (FACScalibur flow cytometer; BD Bioscience). To detect the expression of the following murine antigens, the MAbs in parentheses were employed: CD4 (L3T4), CD8a (Ly2), CD19 (1D3), CD23 ($FC_\epsilon R11$), CD11b (Mac-1a), CD16/CD32 (Fcγ II/III receptor), CD11c (HL3), PD-1 (J43), PD-L1 (M1H5), and PD-L2 (TY25) (BD Pharmingen). Appropriate FITC-, phycoerythrin-, APC-, or Cy-Chrome-conjugated Ig isotypes of irrelevant specificity were used to control for each experimental MAb. Intracellular cytokine staining (ICCS) of IL-10 was performed by incubating 1×10^6 spleen cells for 5 h with complete medium, 5 U/ml IL-2, and 5 μg/ml brefeldin A (Sigma). After washing with phosphate-buffered

TABLE 1. Microarray RNA expression profiling of LP-BM5-infected B6 mice at 3.5 wpi

Function	Description	Accession no.	Fold increase[a]
Generalized infection related	Melanoma antigen, endogenous ecotropic murine leukemia provirus region	D10049	10.24
	Murine (DBA/2) fragment for gag-related peptide	X05546	2.66
	Monokine induced by IFN-γ	M34815	2.67
LP-BM5-induced hyper-Ig	Germ line IgG1 gene, D-J-C region; 3″ exon for secreted form	V00793	3.78
Unknown role in LP-BM5 infection	PD-1	X67914	2.39
	IL-10	M37897	8.22

[a] Values indicate gene expression in infected B6 mice divided by that in uninfected B6 mice.

saline, extracellular staining for cell surface markers was first performed as described above and then the cells were fixed in 2% formaldehyde and permeabilized with 0.5% saponin, followed by intracellular staining with FITC–anti-IL-10 MAb JES5-16E3. All stained cells were analyzed on a FACScalibur flow cytometer using CellQuest software (BD Bioscience).

Microarray RNA expression profiling. Total RNA was isolated from spleen cells from LP-BM5-infected and uninfected mice using RNeasy kits (Qiagen, Valencia, CA). Subsequent microarray experiments were conducted at the Norris Cotton Cancer Center Microarray Shared Resource at Dartmouth Medical School. All procedures, including RNA preparation, hybridization, washes, and analysis using the Affymetrix Murine Genome Array u74A, were conducted according to the manufacturer's (Affymetrix, Inc., Santa Clara, CA) directions.

RNA isolation and real-time quantitative reverse transcription (RT)-PCR. Viral load was determined for BM5def and BM5eco as previously described (12, 20, 24, 41, 42). Briefly, total RNA was isolated from spleen tissue using Tri-Reagent (Molecular Research Center, Cincinnati, OH) and treated with a DNA-free kit (Ambion, Austin, TX). Following RT and amplification of cDNA (Bio-Rad iScript cDNA synthesis kit), PCR was performed using iQ SYBR green Supermix and iCycler software (Bio-Rad, Hercules, CA).

RESULTS

Expression of PD-1, PD-L1, and PD-L2 in uninfected versus LP-BM5-infected C57/BL6 mice. To gain further insight into possible inhibitory molecular pathways involved in LP-BM5-induced disease, WT B6 mice infected with LP-BM5 were sacrificed at 3.5 wpi, a point within the time span we had previously defined by in vivo anti-CD154 MAb blocking experiments as critical for CD154/CD40 interactions and commitment to disease progression (21, 22). Utilizing splenic mRNA obtained from these mice, mRNA expression profiling was performed via an Affymetrix Murine Genome Array (see Materials and Methods) comparison of uninfected versus 3.5-wpi samples as summarized in part in Table 1. Compared to uninfected mice, as expected, the following two classes of genes were highly up-regulated in response to LP-BM5 infection: (i) several commonly expressed sequences as a consequence of LP-BM5 infection per se—e.g., mRNA corresponding to endogenous ecotropic murine leukemia proviral sequences (encoding a melanoma-associated retroviral antigen or a gag-related peptide), presumably cross-reactive with the LP-BM5 retrovirus also of endogenous derivation, and (ii) the germ line IgG1 gene and other Ig-associated sequences, as indicators of LP-BM5-induced hyper-Ig, which is an early activation disease parameter first easily measurable at 3.5 wpi. In addition, other genes without an obvious, or previously described, function in LP-BM5-induced disease were also found to be highly expressed, including those encoding PD-1 and IL-10. Real-time RT-PCR (12), using specific primers, confirmed the increased levels of mRNA for both PD-1 and IL-10 in 3.5-week LP-BM5-infected B6 mice, compared to uninfected control mice (data not shown).

Flow cytometric analyses of spleen cells from 3.5- and 10-week LP-BM5-infected B6 mice were performed to evaluate, at the protein level, the relative cell surface expression of PD-1 (Fig. 1A), PD-L1 (Fig. 1B), and PD-L2 (data not shown). At 3.5 wpi, there was a trend toward increases in the percentages of each of the $CD4^+$, $CD8^+$, $CD19^+$, and $CD11b^+$ cell subsets expressing PD-1 (with that for $CD4^+$ T cells of particularly significance), compared to the low percentages of detectable PD-1 for each of these subsets from uninfected mice. At 10 wpi, significant increases in PD-1 expression were observed in all of these cellular subsets (Fig. 1A). Generally, only small, if any, increases in the mean fluorescence intensity (MFI) were detected for the PD-1-expressing cell populations at 3.5 wpi. At 10 wpi, the MFI values were somewhat increased for all subsets at about 1.5-fold that of analogous cells from the uninfected mice (Fig. 1 legend). Regarding PD-L1, all of the cell subsets (Fig. 1B) appeared to exhibit LP-BM5 infection-dependent up-regulated expression at 3.5 wpi, although the increases in the percent positive cells were statistically significant for only $CD8^+$ T cells and $CD19^+$ B cells, presumably in part due to the widely expressed constitutive levels of PD-L1 (>90%) for each splenic cell subset from uninfected mice. With regard to the MFI of PD-L1 expression, at both 3.5 and 10 wpi, the infection-dependent increases, if any, were relatively modest (i.e., twofold or smaller) for all cell subsets. Only a small percentage of PD-$L2^+$ cells was detectable, and only at 10 wpi with LP-BM5 and only for $CD11b^+$ cells (data not shown). Therefore, cell surface PD-1 protein was expressed at substantially increased levels during LP-BM5-induced disease. PD-L1 expression was also up-regulated above constitutive levels as early as 3.5 wpi with LP-BM5, in contrast to PD-L2. Thus, these collective results are consistent with the possibility of an involvement of PD-1, and in particular PD-L1, in LP-BM5-induced disease.

LP-BM5 retrovirus-infected PD-1 KO mice demonstrated greatly enhanced pathogenesis compared to infected WT mice. To evaluate LP-BM5-induced disease susceptibility, the following standard disease readouts, as previously described and utilized by our and other laboratories (3, 8, 10, 11, 20–24, 26, 28, 41, 42, 47, 73, 74), were evaluated postinfection with LP-

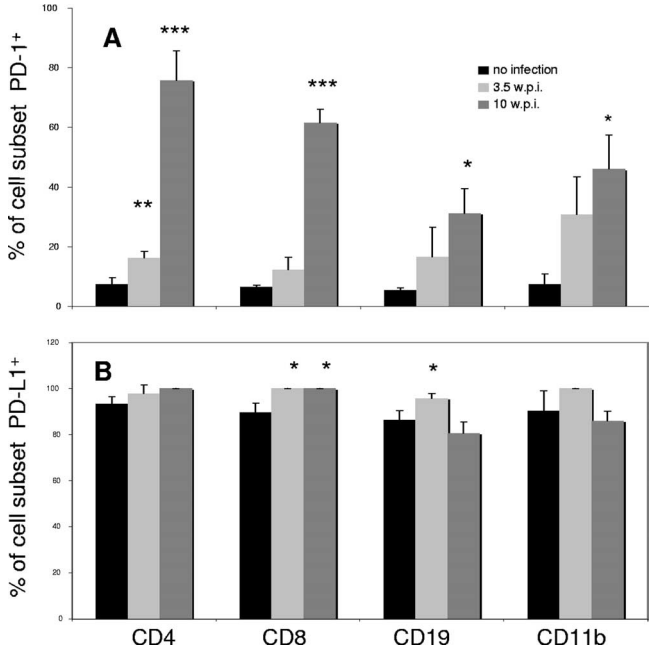

FIG. 1. Upregulated cell surface expression of PD-1 and PD-L1 by spleen cells from LP-BM5-infected B6 mice. Spleen cells from noninfected mice (black bars) and WT B6 mice infected with 5×10^4 PFU LP-BM5 at 3.5 wpi (light gray bars) and 10 wpi (dark gray bars) were stained with MAbs directed to PD-1, PD-L1, or one of the listed cell surface markers. Data shown are the percentages of cells positive for PD-1 (A) or PD-L1 (B) among the total cells of each marker-defined (i.e., CD4, CD8, CD19, or CD11b) subset. MFI values for the spleen cell subsets from uninfected and LP-BM5-infected mice were, respectively, as follows: (3 wpi, PD-1$^+$) CD4$^+$, 16 and 19; CD8$^+$, 15 and 15; CD19$^+$, 42 and 42; CD11b$^+$, 20 and 16; (3 wpi, PD-L1$^+$), CD4$^+$, 17 and 34; CD8$^+$, 18 and 31; CD19$^+$, 67 and 67; CD11b$^+$, 22 and 28; (10 wpi, PD-1$^+$) CD4$^+$, 39 and 60; CD8$^+$, 34 and 55; CD19$^+$, 29 and 47; CD11b$^+$, 33 and 50; (10 wpi, PD-L1$^+$), CD4$^+$, 26 and 43; CD8$^+$, 24 and 41; CD19$^+$, 24 and 35; CD11b$^+$, 35 and 48. This pattern of results was also observed in two other experiments. Significance levels: *, $P < 0.05$; **, $P < 0.01$; ***, $P < 0.001$.

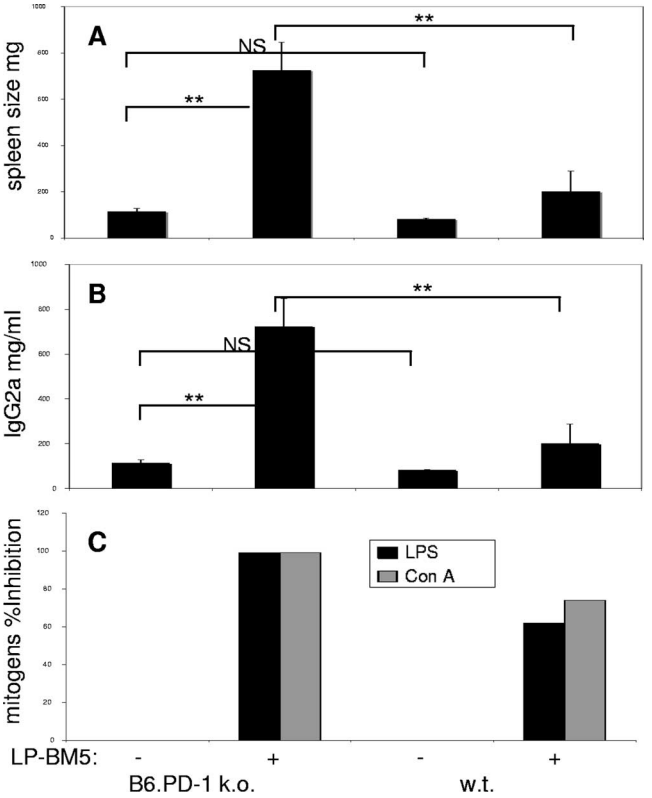

FIG. 2. B6.PD-1 KO mice are more susceptible to LP-BM5-induced disease than WT mice as a function of the viral dose. A somewhat limiting dose of 2×10^4 PFU of LP-BM5 virus was administered to B6.PD-1 KO and WT B6 mice. At 8 wpi, viral pathogenesis was assessed by splenomegaly (A), serum IgG2a levels (B), and the spleen cell mitogenic response to LPS or ConA stimulation (C); the latter is depicted as percent inhibition of the uninfected control LPS and ConA responses. This pattern of results was also observed in one other experiment. Significance levels: NS, $P > 0.05$; *, $P < 0.05$; **, $P < 0.01$.

BM5: splenomegaly (spleen weight) and serum IgG2a concentration (as a measure of hyper-Ig)—both indicators of the early activational aspects of disease; splenic B-cell responsiveness to lipopolysaccharide (LPS) and T-cell responsiveness to concanavalin A (ConA) mitogen stimulation, as indicators of immune system functional status; and characteristic cell surface marker-defined lymphoid subset prevalence. First, it was important to determine whether B6.PD-1 KO mice displayed intrinsic phenotypic differences compared to WT B6 mice that would complicate the assessment of disease by these parameters. However, this was not the case; B6.PD-1 KO versus WT B6 uninfected mice had no statistically significant differences in disease parameter baseline levels—e.g., spleen weight and serum IgG2a levels (Fig. 2), and their spleen cells responded similarly to ConA and LPS mitogen stimulation. PD-1 KO mice infected for 8 weeks with 2×10^4 PFU LP-BM5, a somewhat limiting dose (see below), consistently demonstrated a substantially greater degree of LP-BM5-induced disease by all of the disease readouts examined, compared to WT mice infected in parallel (Fig. 2A and B). For example, the average spleen weight of the infected PD-1 KO mice exhibited a highly significant ($P < 0.001$) approximately sevenfold increase, compared to uninfected KO spleen weight, whereas for WT B6 mice the increase was only about twofold. Similarly, the increase in serum IgG2a concentration for the infected PD-1 KO mice was highly significant, approximately 15-fold, compared to uninfected KO values, in contrast to only about a 2-fold increase for infected versus uninfected WT mice. Consistent with these results but in terms of immunodeficiency readouts, the spleen cell mitogenic responses to LPS and ConA of PD-1 KO cells were essentially completely inhibited, whereas these same responses of infected WT mice demonstrated only partial immunodeficiency; the B-cell response to LPS was inhibited 62%, and the T-cell response to ConA was inhibited 74%.

PD-1 KO and WT mice were also infected with a lower, very limiting dose of LP-BM5 (3×10^2 PFU) and were similarly evaluated at 8 wpi for LP-BM5-induced disease (data not shown). The average spleen size and serum Ig concentration of PD-1 KO mice, albeit with considerable mouse-to-mouse variation, were both approximately fivefold higher than the average responses of uninfected KO mice versus only about a twofold increase for infected WT mice. For the mitogen responses measuring the extent of immunodeficiency, the percent inhibition of responsiveness was partial (74% for LPS,

48% for ConA), owing to the limited viral dose, for PD-1 KO mice. However, substantially less immunodeficiency was observed in infected WT B6 mice—30% less than that of B6.PD-1 KO mice.

Infection of B6.PD-1 KO and WT mice with a high dose 5×10^4 PFU LP-BM5, relative to the experiments of Fig. 2, and evaluation at the extended time point of 10 wpi for LP-BM5-induced disease allowed assessment of whether (i) the absence of PD-1 continued to simply magnify disease symptomatology, irrespective of the viral dose, or (ii) the extent of the effect of the KO of PD-1 on disease was ultimately limited. With this increased dosage of virus and 2 additional weeks of infection, infected PD-1 KO and WT mice had similar mean spleen weights that were not significantly different (data not shown; PD-1 KO mice, 650 mg; WT B6 mice, 720 mg) and both LPS and ConA mitogenic spleen cell responses were completely inhibited in both the KO and WT strains. The only disease readout showing a substantial difference was that for serum IgG2a, as a measure of hyper-Ig, with average values for PD-1 KO and WT B6 mice of 4.9 and 2.3 mg/ml, respectively.

As a function of time postinfection, LP-BM5-infected B6.PD-1 KO mice develop greater retrovirus-induced pathogenesis than LP-BM5-infected WT B6 mice. We next examined the question of whether infected B6.PD-1 KO mice displayed more rapid kinetics of LP-BM5-induced disease compared to WT B6 mice. As shown in Fig. 3A, as early as 3.5 wpi with 2×10^4 PFU LP-BM5 virus, PD-1 KO mice developed significant splenomegaly, with an average spleen weight about five times the mean uninfected spleen weight. At this same early time point postinfection, there was an insignificant increase in spleen weight in WT LP-BM5-infected mice. At the standard terminal 8 wpi, statistically significant (about fourfold) splenomegaly was observed, as expected for infected WT B6 mice, but for infected PD-1 KO mice, much exaggerated disease was observed—a highly significant increase of approximately 10-fold. Indeed, there was a very clear reproducible difference in the spleen weights of PD-1 KO versus WT B6 infected mice when they were compared directly ($P < 0.0001$). Similarly, at 3.5 wpi (Fig. 3B), the average serum IgG2a concentration was also much more significantly ($P < 0.0001$) elevated in LP-BM5-infected PD-1 KO mice, at approximately 25-fold that of uninfected values, than in infected WT mice (~10-fold). At 8 wpi, the PD-1 KO average serum IgG2a value was very exaggerated at ~200-fold that of uninfected KO mice, in contrast to the increase in infected WT mice (~20-fold). Again, for both 3.5- and 8-wpi mice, as with the other activational disease parameters, PD-1 KO mice demonstrated clearly enhanced susceptibility to LP-BM5-induced retroviral disease.

In parallel, spleen cells from LP-BM5-infected PD-1 KO mice are much more severely impaired at the early 3.5-wpi time point in responding to stimulation with the B-cell mitogen LPS and the T-cell mitogen ConA, with essentially complete inhibition of responses to both mitogens. In contrast, these same responses of infected WT B6 mice were inhibited only 33% and 23% after LPS and ConA stimulation, respectively (Fig. 3C). By 8 wpi, although the inhibition of the WT response to ConA had caught up to the continued nearly complete inhibition already observed for the PD-1 KO mice at 3.5 wpi, the immunosuppression of the LPS response continued to lag in these WT infected mice (68% inhibition). Thus, all of the disease parameters measured were consistent in demonstrating that the kinetics of LP-BM5-induced immunodeficiency is greatly accelerated in B6.PD-1 KO, compared to WT B6, infected mice.

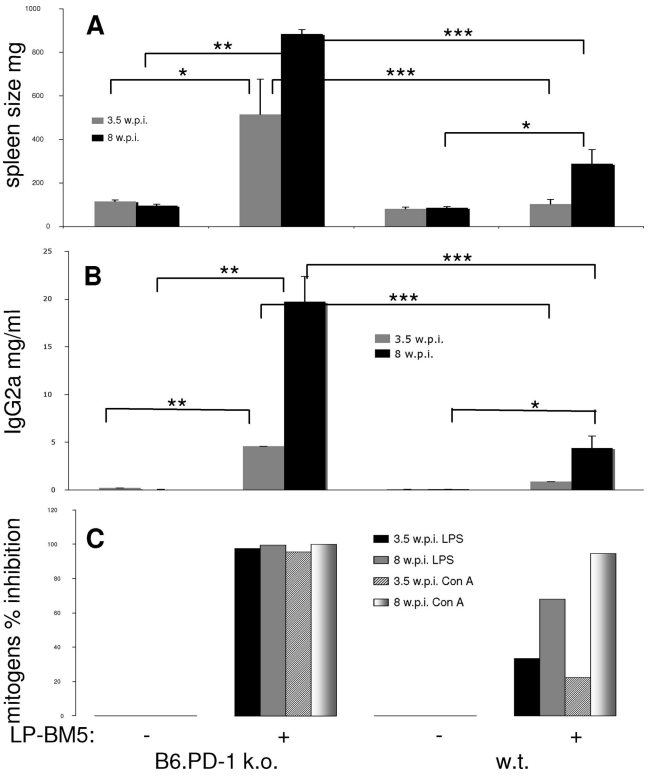

FIG. 3. LP-BM5-infected B6.PD-1 KO mice have detectable LP-BM5-induced disease as early as 3.5 wpi and exaggerated disease compared to WT mice at 8 wpi. For PD-1 KO mice compared to B6 WT mice infected with 2×10^4 PFU LP-BM5 virus, virus-induced disease was assessed by splenomegaly (A), serum IgG2a levels (B), and the spleen cell mitogenic response to LPS or ConA stimulation (C); the latter is depicted as percent inhibition of the uninfected control response. This pattern of results was also observed in three other experiments. Significance levels: *, $P < 0.05$; **, $P < 0.01$; ***, $P < 0.001$.

Infection of B6.PD-1 KO mice with LP-BM5 leads to more pronounced changes in the spleen cell surface expression of CD19 and CD11b. LP-BM5-induced pathogenesis in B6 mice is closely associated with characteristic changes in the expression of specific cell surface molecules that define various cell subsets, including the presence of $CD19^+$ $CD23^+$ B cells and $CD11b^+$ $CD16/CD32^+$ ($Fc_\gamma R^+$) myeloid cells (20, 35). Our and other laboratories have exploited these changes as additional quantitative measures of the extent of disease. Here, uninfected versus infected (2×10^4 PFU) WT B6 and B6.PD-1 KO mice were sacrificed at 3.5 or 8 wpi and spleen cells were evaluated by flow cytometric analyses (Fig. 4A). As shown in the representative experiment of Fig. 4A, in infected WT mice, as early as 3.5 wpi the percentage of $CD23^+$ $CD19^+$ cells declined, but only slightly (61% to 52% of all splenocytes), while this downward trend continued to 31% at 8 wpi. In sharp contrast, in infected PD-1 KO mice a greatly accelerated decline from the uninfected level of 58% $CD23^+$ $CD19^+$ cells was observed, to only 22% at 3.5 wpi and 17% at 8 wpi. In addition, and strikingly, the decline in the percentage of total $CD19^+$ (Fig. 4B) spleen cells in infected mice

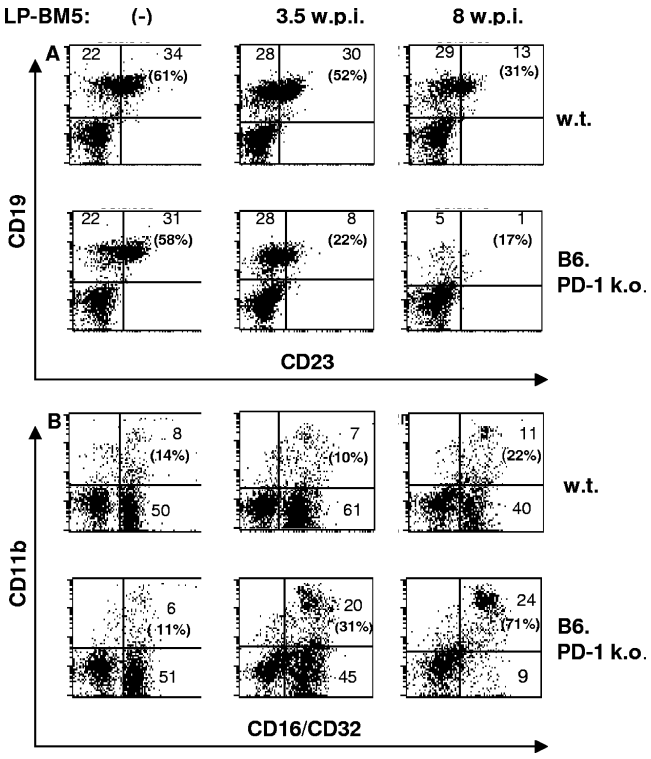

FIG. 4. B6.PD-1 KO mice develop more dramatic spleen cell phenotypic changes than WT B6 mice after LP-BM5 infection. B6.PD-1 KO and WT B6 mice were infected with 2×10^4 PFU LP-BM5 virus and sacrificed at 3.5 or 8 wpi. Spleen cells labeled in two-color analyses with MAb to cell surface markers CD23 and CD19 (A) or CD16/CD32 and CD11b (B) were analyzed on a FACScalibur flow cytometer. The percentages of total $CD19^+$ cells that are also $CD23^+$ are shown in the upper right quadrants of panel A, and the percentages of total CD16/$CD32^+$ cells that are also $CD11b^+$ are shown in the upper right quadrants of panel B. A log fluorescence scale was used. This pattern of results was also observed in two other experiments.

was much sharper and complete in PD-1 KO mice—by 8 wpi, only 6% of the total splenocytes expressed detectable CD19, irrespective of CD23 expression. In terms of total splenic B-cell numbers, in both WT and PD-1 KO infected B6 mice, there was an increase by 3.5 wpi, due to the developing splenomegaly. However, this enlargement of the spleens could not offset the dramatic decline in the percentage of B cells in 8-week-infected PD-1 KO mice—compared to uninfected mice, splenic B-cell numbers were decreased about fivefold. That this change represented an actual loss of B cells, rather than a selective down-regulation of CD19 (as well as CD23), was supported by the corresponding lack of $B220^+$ cells (data not shown) and, as detailed below (in comments concerning Fig. 4B), $CD11b^-$ CD16/$CD32^+$ cells, the phenotype of essentially all conventional B cells.

Another spleen cell phenotypic change in LP-BM5-infected mice involves an increase in $CD11b^+$ CD16/$CD32^+$ myeloid spleen cells (Fig. 4B). In WT mice, this change was first readily apparent at 8 wpi (22% of CD16/$CD32^+$ cells are also $CD11b^+$, versus 14% for uninfected mice). However, in B6.PD-1 KO mice, this phenotypic change was greatly exaggerated; at only 3.5 wpi, an ~3-fold increase was already evident and by 8 wpi, an ~6.5-fold increase was observed, with 71% of the CD16/$CD32^+$ cells also expressing CD11b. As the CD16/CD32-defined FcγR is also expressed on essentially all conventional splenic $CD19^+$ B cells, the corresponding decrease in PD-1 KO mice of the CD16/$CD32^+$ $CD11b^-$ population was consistent with the above-noted decline in B cells as defined as $CD19^+$ (Fig. 4A). Indeed, in all cases the percentages of total $CD19^+$ cells ($CD23^+$ or $CD23^-$) were very close to that of this CD16/$CD32^+$ $CD11b^-$ population. Overall, these results (i) confirmed the exaggerated nature of LP-BM5-induced disease in PD-1 KO mice (by a disease parameter not directly measuring function) and (ii) demonstrated a dramatic (≥80%) loss of splenic B cells compared to WT B6 mice.

B-cell expression of PD-1 is primarily involved in moderating LP-BM5-induced disease in WT B6 mice. PD-1 expression therefore appears important in limiting the kinetics and extent of LP-BM5-initiated disease. To approach the question of which cellular subset(s) is required to express PD-1 to moderate the effects of LP-BM5-induced disease in WT mice, a set of reciprocal adoptive-transfer experiments were undertaken by using highly purified WT, versus PD-1 KO, donor $CD4^+$ T and B cells. Thus, B6.Rag-1 KO recipients were given intravenous parallel transfers of four combinations of purified $CD4^+$ T and B cells, i.e., (i) WT B and $CD4^+$ T cells, (ii) PD-1 KO B and $CD4^+$ T cells, (iii) WT B and PD-1 KO $CD4^+$ T cells, and (iv) PD-1 KO B and WT $CD4^+$ T cells, by using essentially the reconstitution protocol we previously used (23, 41, 42). Three days later, a portion of the recipients were infected with LP-BM5. At sacrifice at 10 wpi, all of the disease parameters measured, including spleen weight, mitogen responsiveness as a measure of immunodeficiency, and the phenotypic shift to increased percentages of $CD11b^+$ CD16/$CD32^+$ cells, were most pronounced (relative to the WT/WT control) under two experimental conditions, (i) PD-1 KO B and PD-1 KO $CD4^+$ T cells and (ii) PD-1 KO B and WT $CD4^+$ T cells (Fig. 5). The observation that LP-BM5-infected Rag-1 KO mice that had previously received PD-1 KO B cells along with either WT or PD-1 KO $CD4^+$ T cells displayed the most disease strongly suggested that it was the common lack of PD-1 expression on B cells that was responsible for the exaggerated virus-induced disease. Said another way, this reproducible pattern of results clearly implied that in LP-BM5-infected WT B6 mice, B-cell PD-1 expression was of primary importance in its moderation of LP-BM5-induced disease.

In vivo blocking studies with anti-ligand MAbs to modulate LP-BM5-induced disease in WT B6 mice. To determine which of the PD-1 ligands, PD-L1 and/or PD-L2 (15, 72), might be involved in the ligation of PD-1 to mediate the down-modulation of virus-induced disease, the following experimental conditions were defined: LP-BM5-infected WT B6 mice were treated in vivo with anti-PD-1 MAb as a positive control for enhanced disease, with anti-PD-L1 MAb, or with anti-PD-L2 MAb (see Materials and Methods). Standard LP-BM5-induced disease readouts were performed at either 3.5 or 8 wpi, including splenomegaly, hyper-Ig, and mitogen responsiveness/immunodeficiency (Fig. 6). At 3.5 wpi, spleen weight comparisons between uninfected B6 mice and LP-BM5-infected mice without versus with antibody treatment indicated that all infected mice had significant splenomegaly. However, although the differences were not statistically significant, there was a trend toward more disease in both the anti-PD-1 (expected, as blocking PD-1 would be analogous to the use of PD-1 KO mice) and anti-ligand (PD-L1 or PD-L2) MAb-treated

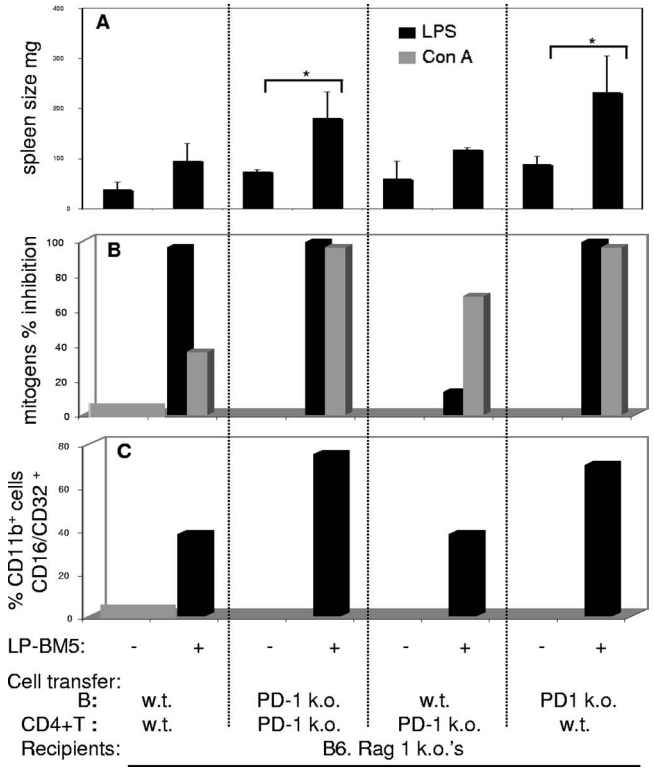

FIG. 5. B-cell PD-1 expression is primarily involved in moderating LP-BM5-induced disease in WT B6 mice. Rag-1 KO B6 mice were reconstituted with purified cellular subsets obtained from either WT or PD-1 KO donors, and 3 days after such adoptive transfer, recipients were infected with 1×10^5 PFU LP-BM5 virus. At 10 wpi, all mice were evaluated for disease severity by disease readouts measuring either spleen size (A) or mitogen reactivity (B); the latter is depicted as percent inhibition of the uninfected control response. The percentages of recipient $CD11b^+$ cells that are CD16/CD32 at the time of sacrifice are shown in panel C. This pattern of results was also observed in one other experiment. Significance level: *, $P < 0.05$.

mice (Fig. 6A). A similar pattern of results was obtained when assessing the extent of LP-BM5-induced disease at 3.5 wpi by means of the hyper-Ig and mitogen responsiveness readouts (Fig. 6B and C), with the suggestion of somewhat augmented disease observed for either anti-PD-L1 or anti-PD-L2 (or anti-PD-1) MAb-treated, infected mice, although again the differences were not statistically significant compared to mice infected but not receiving anti-PD-L MAb treatment. For example, the serum Ig concentrations of anti-PD-1-, anti-PD-L1-, or anti-PD-L2-treated mice at 3.5 wpi were all two- to threefold that of infected, untreated mice. In contrast, at 8 wpi, only those mice that were LP-BM5 infected and treated with the anti-PD-L1 MAb consistently developed a substantially exaggerated, statistically significant degree of disease compared to infected but otherwise untreated mice (e.g., spleen weight, $P < 0.05$; serum IgG2a, $P < 0.05$) (Fig. 6A and B). This differential result for blocking by anti-PD-L1 versus anti-PD-L2 MAb was observed for all disease parameters, except for the single readout of responsiveness to the B-cell mitogen LPS, where anti-PD-L2 treatment also led to enhanced hyporesponsiveness. Indeed, at 8 wpi, noting the different *y*-axis scales for the splenomegaly and hyper-Ig parameters compared to 3.5 wpi (Fig. 6A and B), all disease readouts indicated that the largest absolute enhancement of viral pathogenesis was observed following anti-PD-L1 treatment of LP-BM5-infected mice.

In summary, these data confirm the results obtained with the PD-1 KO mice (Fig. 2 to 5) and further suggest that, particularly for full disease measured at 8 wpi, PD-1-dependent moderation of virus-induced disease involves preferential ligation of PD-1 by PD-L1.

B6.IL-10 KO mice also display exaggerated viral pathogenesis after LP-BM5 infection. Based on the expression-profiling data on genes induced after LP-BM5 infection (Table 1) and reports linking occupancy of PD-1 by PD-L1 and the production of IL-10 (15, 38, 65, 68), we next investigated whether IL-10 might also be down-regulating disease in WT B6 mice. IL-10 KO mice infected with 2×10^4 PFU LP-BM5, similar to PD-1 KO mice given this same dose, exhibited a more exaggerated form of disease at 8 wpi, based on all measured disease parameters, including splenomegaly, hyper-Ig, and mitogen responsiveness as an indication of immunodeficiency (Fig. 7). For example, IL-10 KO mice developed an about sixfold increase, compared to uninfected spleen weight, whereas when this same comparison was made for uninfected and infected WT mice, a substantial but only about threefold increase in spleen size was observed (Fig. 7A). The average increased serum IgG2a level for infected IL-10 KO mice was also substantially higher, at approximately 130-fold, compared to an ~30-fold increase for WT mice infected in parallel. Similarly, both the LPS and ConA mitogen responses of infected IL-10 KO mice were almost totally inhibited, while the inhibition of the LPS and ConA responses was less pronounced in infected WT mice (77% and 94%, respectively).

When B6 versus B6.IL-10 KO mice were infected instead with the very limiting dose of 3×10^2 PFU LP-BM5, the same pattern of exaggerated disease for IL-10 KO mice was observed (data not shown). For example, despite some mouse-to-mouse variation (as expected at this low dose [see above]), infected IL-10 KO mice had with an average spleen weight of 470 mg versus only 140 mg for WT mice infected in parallel. Similarly, for average serum IgG2a values of infected mice, the response, though considerably lower than at the 2×10^4 dose, was substantial and noticeably skewed to more disease in the IL-10 KO mice, with a mean value of 4 mg/ml versus 330 μg/ml for WT B6 mice. With respect to mitogen responsiveness, a similar trend was observed, particularly for the ConA response, which was inhibited 88% in IL-10 KO mice versus only 43% inhibition in WT infected mice.

Thus, at two different virus doses, LP-BM5-infected B6.IL-10 KO mice, compared to WT mice, developed more severe splenomegaly, hyper-Ig, and immunodeficiency—a phenotype analogous to that of mice in which the PD-1 pathway was inhibited either by use of PD-1 KO mice or via the anti-PD-1 or anti-PDL MAb blocking approach.

LP-BM5-infected IL-10 KO mice were also more susceptible than WT mice to LP-BM5-induced disease at the early time point of 3.5 wpi, with a highly significant average spleen weight ($P < 0.001$) of 380 mg (more than fivefold that of uninfected mice), whereas there was a much smaller increase in the spleen weight of infected WT mice, i.e., 177 mg (1.8-fold compared to uninfected WT mice). Serum IgG2a levels followed the same pattern of greater hyper-Ig in IL-10 KO mice ($P < 0.001$), with IL-10 KO

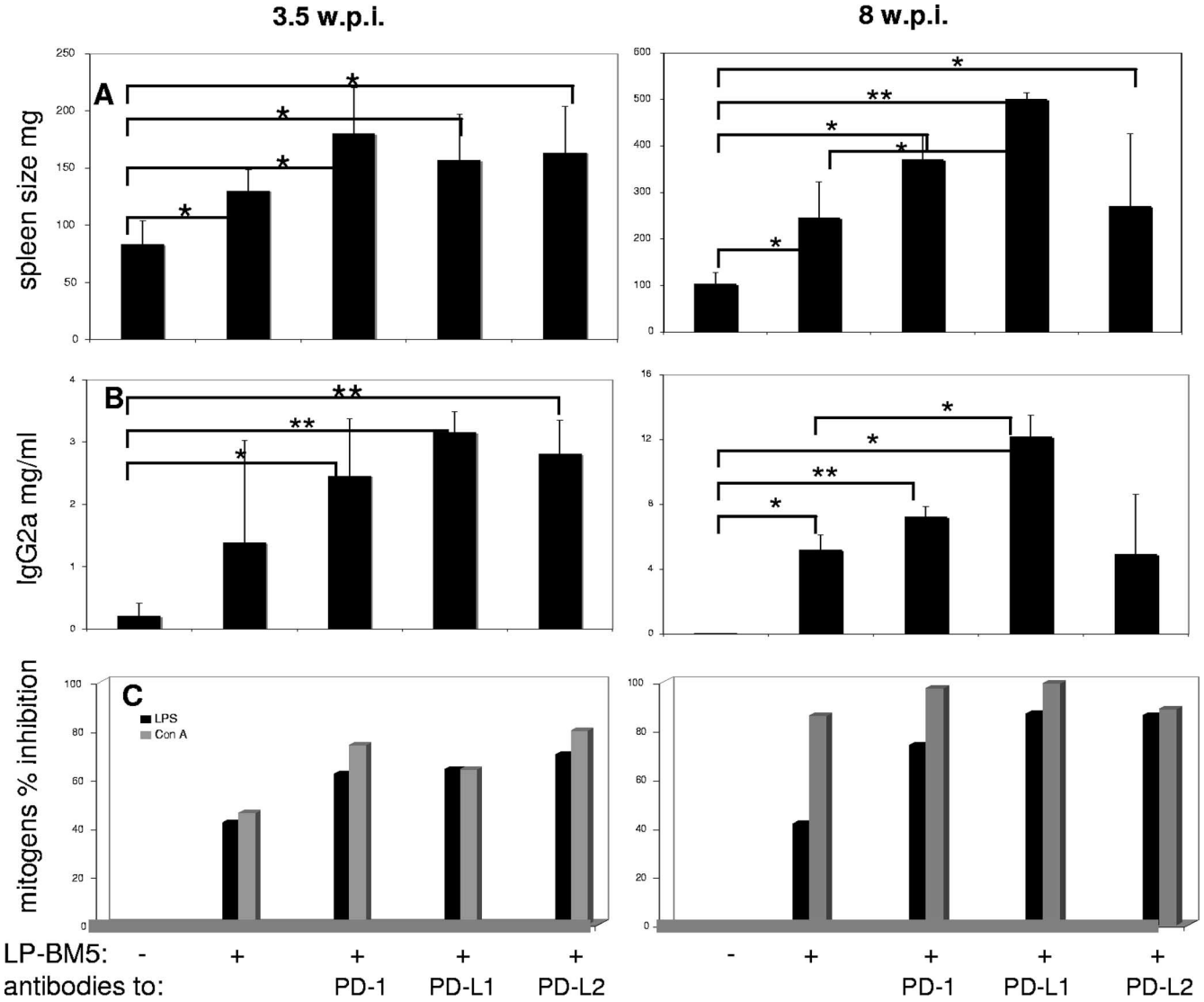

FIG. 6. PD-L1, rather than PD-L2, appears to be the preferential ligand for PD-1 in LP-BM5-induced disease, at least at 8 wpi. WT B6 mice were infected with 2×10^4 PFU LP-BM5 virus and given anti-PD-1, anti-PD-L1, and anti-PD-L2 MAbs intraperitoneally three times per week for either 3 or 7.5 weeks. At the termination time point of 3.5 or 8 wpi, LP-BM5-induced disease was evaluated by spleen weight (A), serum IgG2a ELISA (B), and mitogen response to LPS and ConA stimulation (C); the latter is depicted as percent inhibition of the uninfected control responses. With respect to the data for spleen weights and serum IgG2a levels, at the 3.5 wpi time point, comparing the untreated and anti-PD-1, anti-PD-L1, or anti-PD-L2 MAb-treated mouse groups, all comparisons were not statistically significant ($P \geq 0.05$). In contrast, at 8 wpi, the untreated versus anti-PD-L1 MAb-treated comparison was significant ($P < 0.05$). All other comparisons were not statistically significant. Significance levels: *, $P < 0.05$; **, $P < 0.01$.

mice averaging 3.1 mg/ml (>45-fold, compared to uninfected mice) and WT mice 1.5 mg/ml (>25-fold compared to uninfected mice, with one WT mouse not yet exhibiting obvious hyper-Ig). The response to the T-cell mitogen ConA was also 90% inhibited for IL-10 KO mice at 3.5 wpi versus a fully intact response for infected WT B6 mice. IL-10 KO mice were also similar to infected PD-1 KO mice (Fig. 4) at 3.5 wpi with LP-BM5, as infection led to IL-10 KO spleen cell preparations that exhibited (i) a trend toward an increase in $CD11b^+$ CD16/$CD32^+$ cells (a 33% rise, borderline significant at $P < 0.07$) and (ii) a decrease in $CD19^+$ $CD23^+$ B cells (an ~46% decline, $P < 0.001$).

Thus, based on these cumulative results and the mRNA expression data in Table 1, it appeared that in WT LP-BM5-infected B6 mice, as a consequence of IL-10 expression, viral disease was decreased. As it is well known that a wide variety of cell types are capable of secreting IL-10, it was of interest to determine the identity of the cells responsible for IL-10 production in WT B6 mice following infection by LP-BM5 retrovirus. By ICCS analysis coupled with cell surface labeling with MAbs directed to CD4, CD8, B220 (for B cells), CD11b (for myeloid cells), and CD11c (for DC), ex vivo splenic cells were assessed at both 3.5 and 8 wpi (Fig. 8). Compared to uninfected B6 mice, where the percentage of IL-10-producing cells among these subsets was undetectable, except for 0.9% of $CD11b^+$ cells, LP-BM5 infection led to an increased percentage of IL-10 producers. Namely, ~4-fold (3.5 wpi, $P < 0.05$) to

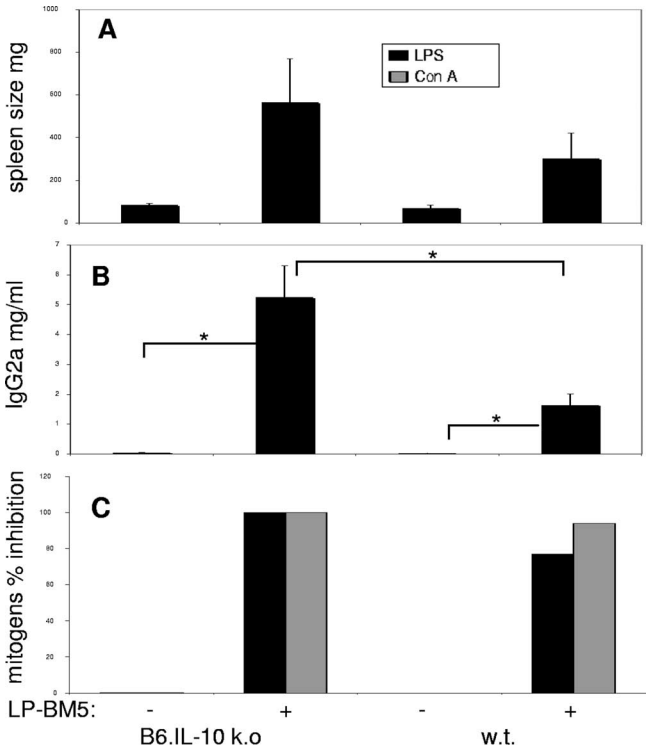

FIG. 7. IL-10 KO B6 mice are more susceptible to LP-BM5-induced disease than WT B6 mice. IL-10 KO and WT B6 mice were infected with 2×10^4 PFU LP-BM5 and sacrificed at 8 wpi. Mice were evaluated for splenomegaly, serum Ig levels, and spleen cell responses to LPS and ConA; the latter is depicted as percent inhibition of the uninfected control response. This pattern of results was also observed in one other experiment. Significance level: *, $P < 0.05$.

~5.4-fold (8 wpi, $P < 0.001$) expansions of IL-10-producing cells were observed, and this occurred entirely within the $CD11b^+$ subset (Fig. 8). Based on the lack of a corresponding increase among $CD11c^+$ cells (Fig. 8), and given preliminary experiments with anti-F4/80 staining, it appeared that macrophage or macrophage-like cells were primarily, if not solely, responsible for the LP-BM5 induction of IL-10 production.

The results from Fig. 8, taken together with the very similar exaggerated disease phenotypes of the IL-10 KO and PD-1 KO strains following LP-BM5 infection, suggested that the PD-1 and IL-10 pathways might be linked mechanistically. As a first approach toward testing this possibility, we also examined IL-10 production in infected PD-1 KO mice. The $CD11b^+$ macrophage-like population again appeared to be primarily, if not solely, responsible for IL-10 production in PD-1 KO mice. However, in contrast to B6 mice (Fig. 8), an LP-BM5 infection-dependent increase in the percentage of ($CD11b^+$) cells producing IL-10 by ICCS analysis was not observed at either 3.5 wpi ($P \geq 0.05$) or 8 wpi ($P \geq 0.05$) (Fig. 9). This lack of increased IL-10 production was underscored by the observation that the expansion of the $CD11b^+$ macrophage-like population was even greater (about twofold) in the PD-1 KO, compared to WT B6, infected mice (confirming the results of Fig. 4). Similarly, when IL-10 expression was assessed instead by enzyme-linked immunospot assay analysis, again, the LP-BM5 infection-dependent increase in IL-10-secreting cells observed with WT B6 mice was not detected in PD-1 KO mice (data not shown). Thus, the inability of LP-BM5-infected PD-1 KO mice to express increased IL-10 in the $CD11b^+$ compartment was consistent with a "linear relationship" between PD-1

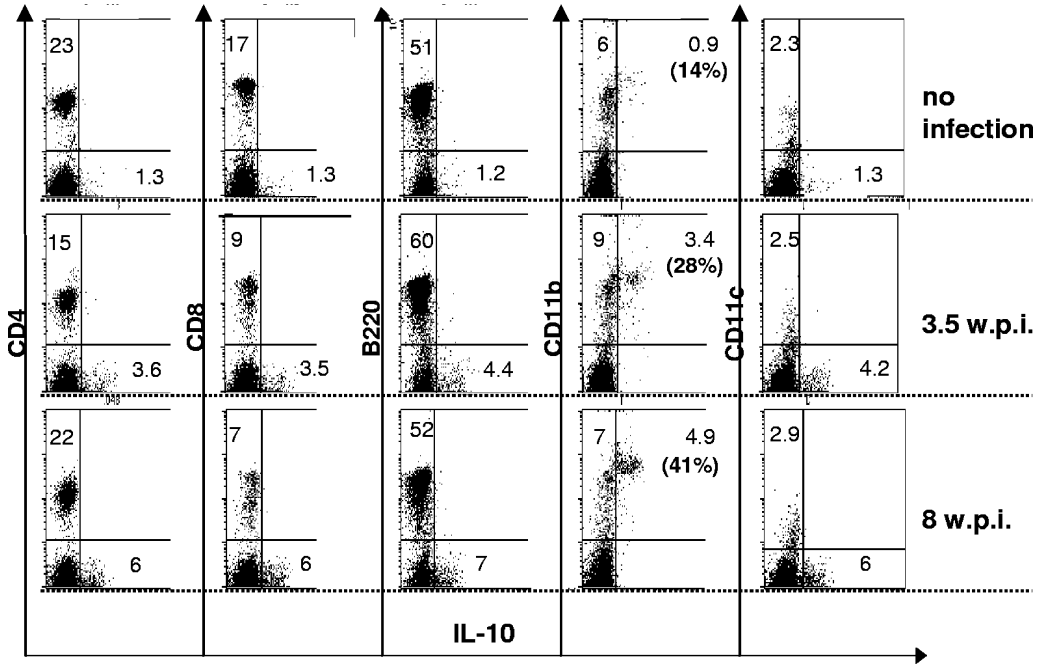

FIG. 8. LP-BM5 infection of WT B6 mice induces an increase of $CD11b^+$ IL-10^+ spleen cells. Spleen cells from uninfected WT B6 mice versus LP-BM5-infected (2×10^4 PFU) WT B6 mice at 3.5 or 8 wpi were labeled with APC-conjugated MAbs to the indicated cell surface markers with subsequent ICCS for IL-10 (see Materials and Methods). The labeled cells were analyzed on a FACScalibur flow cytometer using CellQuest software (BD Bioscience). The significance levels for the percentage of $CD11b^+$ IL-10^+ spleen cells from infected versus uninfected mice were as follows: 3.5 wpi mice, $P < 0.05$; 8 wpi mice, $P < 0.001$. This pattern of results was also observed in two other experiments.

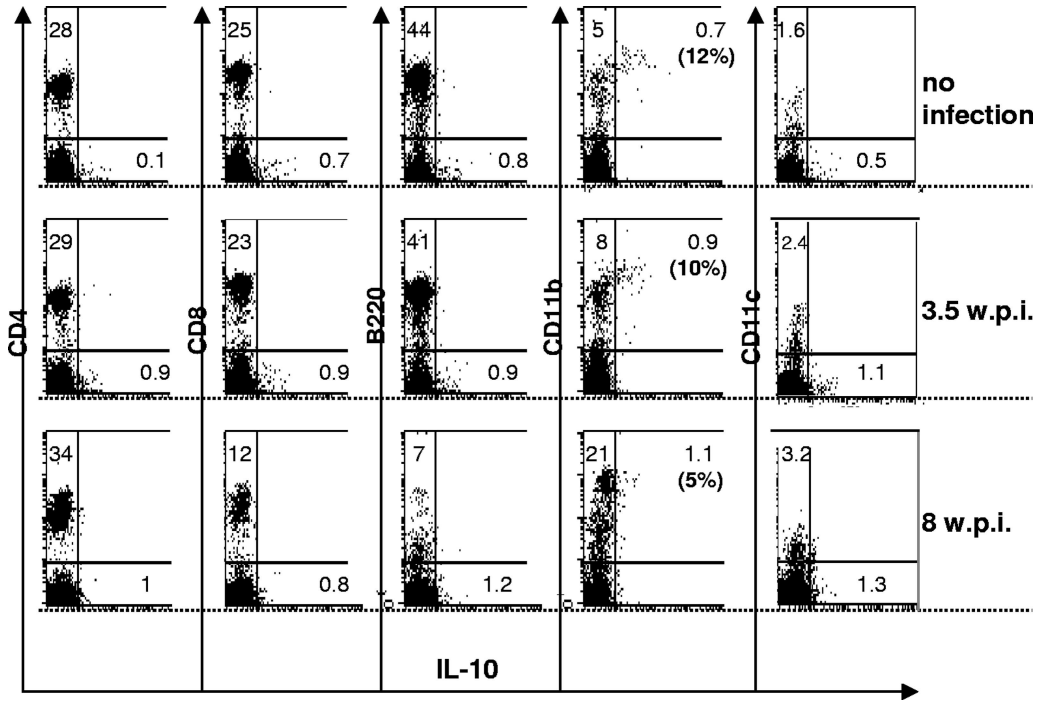

FIG. 9. LP-BM5 infection of PD-1 KO B6 mice does not induce an increase in $CD11b^+$ $IL\text{-}10^+$ spleen cells. Spleen cells from uninfected B6 mice versus LP-BM5-infected (2×10^4 PFU) PD-1 KO B6 mice at 3.5 or 8 wpi were labeled with APC-conjugated MAbs to the indicated cell surface markers with subsequent ICCS for IL-10 (see Materials and Methods). The labeled cells were analyzed on a FACScalibur flow cytometer using CellQuest software (BD Bioscience). The significance levels for the percentage of $CD11b^+$ $IL\text{-}10^+$ spleen cells from infected versus uninfected mice were as follows: 3.5 wpi, $P \geq 0.05$; 8 wpi, $P \geq 0.05$.

and IL-10 in WT B6 mice. These results further suggested that PD-1/PD-L ligation might be the basis for IL-10 production, which then limits the extent of disease in infected B6 mice.

Viral load in infected WT, PD-1 KO, and IL-10 KO mice. To determine if the exaggerated disease observed with LP-BM5-infected PD-1 and IL-10 KO mice was simply due to an enhanced ability of the component retrovirus types to infect and spread in these different hosts, compared to WT B6 mice, we performed real-time, quantitative RT-PCR assays for both the BM5def (pathogenic defective) and BM5eco (helper) retroviruses, as we have previously established (12). Although there was some variation from experiment to experiment in the absolute levels of retroviral RNAs detected, in multiple analyses we could find no evidence for any consistent differences in viral load among B6 versus PD-1 KO versus IL-10 KO strains (data not shown). A lack of significant difference in retroviral RNA expression was observed at both 3.5 and 8 wpi. Thus, the pronounced degree of disease in infected PD-1 and IL-10 KO mice did not appear to be related to substantial differences in BM5def or BM5eco expression.

DISCUSSION

The results of the present study highlight the fine balance of T-cell responses in mediating protective immunity and also, frequently, a substantial portion of the virus-induced immunopathogenesis that is characteristic of many viral infections. Thus, especially in many chronic viral infections (e.g., lymphocytic choriomeningitis in mice; hepatitis B, hepatitis C, and HIV/AIDS in humans; etc.), T-cell responses in particular, by causing bystander tissue damage in an (often unsuccessful) attempt to eradicate or contain the virus, constitute a double-edged sword. If the virus or virus-infected cells cannot be cleared entirely or quickly, a continuing source of viral antigen often leads to dysregulated T-cell responses that are not fully effective against the virus yet paradoxically are sufficient over time to seriously damage host tissues.

Recently, in several chronic viral infection systems there have been concerted efforts to boost protective T-cell responses. Rather than attempting to enhance antiviral T-cell immunity by interventions focused on the cytokines and receptor-ligand pairs that promote the generation of specific $CD8^+$ T cells (such as CD28:CD80/CD86, IL-12, etc., that mediate costimulation), these new approaches have targeted negative regulatory pathways. In particular, interruption of the ligation of PD-1 on activated $CD8^+$ (and $CD4^+$ helper) T cells by PD-L1 (PD-L2) has shown promise in stabilizing or reversing the progressive $CD8^+$ T-cell dysfunction characteristic of chronic viral infections (e.g., see references 5, 14, 19, 31, 55, 65, 69, and 70). For example, in LCMV clone 13 (LCMV-13) chronic infection in mice, in vivo MAb blockade of PD-1/PD-L1 interactions can at least partially circumvent the characteristic exhaustion of the LCMV-specific $CD8^+$ T-cell response (5).

Similarly, in humans the analogous exhaustion of the hepatitis C virus-specific $CD8^+$ T-cell compartment was counteracted by anti-PD-L1 antibody treatment, and T-cell function was thus restored (70). In addition, and as a retroviral infection of particular relevance to the present study, a series of recent

papers has provided evidence of a central role for PD-1/PD-L-mediated down-modulation of the anti-HIV type 1 (HIV-1) $CD8^+$ T-cell response (14, 19, 55, 69). For example, in HIV-seropositive individuals, activated $CD8^+$ T cells directed to HIV-1 (and other persisting viruses, notably, Epstein-Barr virus, which causes chronic virus infection[s]), but not those specific for acutely infecting viruses such as vaccinia virus, exhibited up-regulated PD-1 expression. In addition, levels of PD-1 expression have been associated with decreased in vitro proliferative responses of $CD8^+$ T cells to HIV antigenic stimulation, decreased $CD4^+$ T-cell counts, and increased viral loads, suggesting that the degree of PD-1 expression correlates directly with the severity of virus-induced disease (14). In vitro approaches to block the ligation of PD-1 led to at least a partial restoration of specific $CD8^+$ T-cell numbers and functions, i.e., proliferation, lytic-component (granzyme B) expression, and cytokine production (69). Conversely, using polyclonal anti-PD-1 antibody in a cross-linked, presumably stimulatory, form resulted in decreased HIV-1 antigen-specific T-cell proliferation (55).

The negative regulatory IL-10 cytokine has also received much recent attention as a target for interventions to improve protective antiviral immunity. For example, of particular relevance to the present discussion of chronic viral infections, recent studies by two groups have identified a critical role for the IL-10/IL-10R pathway in the LCMV-13 chronic infection system (7, 17). First, IL-10 secretion is substantially increased during this chronic infection, which presumably contributes to the dysregulation of the protective $CD8^+$ T-cell antiviral response. Second, by treating with a blocking anti-IL-10R antibody soon after infection of mice with LCMV-13 or by use of IL-10 KO mice, the infection-dependent down-regulation of LCMV-specific $CD8^+$ (and $CD4^+$) T-cell responses, including gamma interferon (IFN-γ) and tumor necrosis factor alpha production, was restored. Moreover, with interruption of the IL-10/IL-10R pathway, viral titers were substantially reduced and there was a timely resolution of the chronic infection. Interestingly, in light of the possible intersection of the IL-10/IL-10R and PD-1/PD-L negative regulatory pathways, anti-IL-10R antibody treatment led to a substantial reduction in the percentages of $PD\text{-}1^+$ anti-LCMV-13-specific $CD4^+$ and $CD8^+$ T cells in chronically infected mice (17).

Positive effects on protective T-cell immunity can thus be achieved by interfering with these negative regulatory pathways. An added benefit may be a concomitant decrease in virus-induced immunopathology. For example, in the LCMV-13 virus chronic infection system, blocking the occupancy of PD-1 by specifically anti-PD-L1 MAb treatment restored $CD8^+$ T-cell immunity and allowed better control of the virus without inducing significant immunopathology (5). The chronic, relatively high viral antigen loads were thus decreased but not eliminated in all tissues by anti-PD-L1 MAb treatment. Assuming that the antibody blocking was thus not complete, such a PD-1/PD-L1 partial blockade may have been a prime factor in tipping the balance to effective immunity yet with decreased immunopathology. Indeed, total interruption of PD-1/PD-L1 interactions clearly exacerbated pathogenesis in LCMV-13-infected mice; while WT mice developed the chronic form of the infection, PD-L1 KO mice died due to overt immunopathology (5). These results underscore the key involvement of PD-L1 (and, by implication, PD-1) in moderating immunopathological, as well as protective, antiviral immune responses.

In the LP-BM5 retroviral system described herein, loss of PD-1 ligation, particularly by PD-L1, at 8 wpi also leads to greatly enhanced viral pathogenesis (Fig. 2 to 4 and 5). We and others have demonstrated that $CD4^+$ T cells (and B cells) are required for LP-BM5-induced disease (10, 23, 48, 73). Further, as we have shown that $CD4^+$ T cells must be able to express CD154 to ligate B-cell CD40 to mediate LP-BM5-initiated disease (21–23), this system illustrates that there is virus co-opting of the immune system for viral pathogenesis and that disease depends on $CD4^+$ T effector cell-mediated direct or indirect immunopathology.

Although our results thus have general similarity to the LCMV-13 system, noteworthy differences appear to account for our observations that interruption of PD-1/PD-L interactions or IL-10 production led only to exaggerated LP-BM5-induced disease, with no evidence of enhanced protective immunity. First, in the prototypic susceptible B6 strain studied here, we have no evidence for a protective $CD8^+$ T-cell response. In disease-resistant BALB/c mice, however, we have shown that CD8-deficient (chronic in vivo anti-CD8 MAb treated or CD8 KO) mice convert to disease susceptibility (27, 45) and that WT BALB/c mice generate a strong antiviral $CD8^+$ T-cell response (63). Indeed, the BALB/c $CD8^+$ T effector cells are highly lytic, secrete IFN-γ, and are protective against LP-BM5 virus challenge in vivo, in terms of both inhibition of disease and the ultimate viral load, after their adoptive transfer into BALB/c. CD8 KO recipients (27, 44). Of note, both the polyclonal and clonal $CD8^+$ T-cell populations that were protective were specific for a unique K^d-presented immunodominant epitope, SYNTGRFPPL, which derives from a previously unrecognized alternative (+1 nucleotide) *gag* translational open reading frame of the LP-BM5 retrovirus (44, 45). In contrast, the same immunization approaches with LP-BM5 virus or viral *gag* vector expression systems were unable to raise LP-BM5 virus-specific $CD8^+$ cytotoxic T lymphocytes in B6, BALB.B congenic, or other $H\text{-}2^b$ susceptible mice (45, 63). Thus, in the apparent absence of evidence of even a suboptimal protective $CD8^+$ T-cell response in B6 mice, interruption of the PD-1 or IL-10 negative regulatory pathway would not have been able to provide the beneficial effect of augmented protective T-cell immunity to LP-BM5. Rather, in contrast to the LCMV-13 and other chronic viral systems described above, release from PD-1 and IL-10 negative control should only have been able to increase the strength of the immunopathogenic $CD4^+$ T-cell response.

A second difference in LP-BM5-infected B6 mice, compared to the reports on the positive effects of PD-1/PD-L1 blockade in LCMV and other chronic virus systems, is the nature of the cell type that critically expresses PD-1. Whereas the focus in these chronic virus systems was on PD-1 expression by the protective $CD8^+$ (or $CD4^+$) T cells, the present cell subset fractionation and reconstitution experiments identified B-cell-expressed PD-1 as crucial for the normal down-modulation of LP-BM5-induced immunopathogenesis in WT B6 mice (Fig. 5). Our identification of B cells as the most relevant cells for PD-1 expression and consequent regulation of the extent of LP-BM5-induced disease is consistent with numerous reports indicating the central role of B cells in this retroviral immu-

nodeficiency model (10, 20, 23, 33, 34, 40, 54, 74). The mechanism of this B-cell-dependent, PD-1-mediated inhibition of LP-BM5-induced disease is unclear. One possibility is a direct effect on B cells in which PD-1-initiated negative signaling or apoptosis of B cells limits disease. If B-cell apoptosis per se is the relevant mechanism, however, in PD-1 KO mice, a higher percentage of B cells would be predicted, not the substantially lower percentages observed after LP-BM5 infection (Fig. 4). Alternatively, enhanced B-cell survival in PD-1 KO mice might not lead to an accumulation of conventional B cells but rather allow, via the extended B-cell life span, for their enhanced further differentiation into "effector B cells"—e.g., memory B, preplasma, and/or plasma cells. This possibility is in keeping with the massive hyper-Ig observed especially in LP-BM5-infected PD-1 KO mice (Fig. 2 and 3). In addition, a favored interpretation of our previous (20) finding that CD154-ligated B-cell CD40 signaling occurs primarily, if not exclusively, through TRAF6—i.e., that LP-BM5 virus-induced disease is minimal in B6.CD40-TRAF6 binding site mutant mice—is that B effector cells are necessary for this retrovirus-mediated disease. Thus, to our knowledge, the only obvious immunological phenotype of these B6.CD40 KO background mice, which express a transgenic chimeric CD40 (human external and mouse transmembrane and cytoplasmic domains) with a mutated TRAF6 site, is a dramatically reduced plasma cell compartment and a related relative inability to produce class-switched IgG1 antibody responses to antigenic stimulation (2).

As a related mechanistic consideration, it is useful to compare the results here of the disease phenotypes of B6 mice infected with LP-BM5 in the context of the absence of the PD-1/PD-L versus the IL-10 negative regulatory pathway. Because the ultimate outcome of greatly exaggerated disease is so similar (Fig. 2 and 3 versus 7), it is tempting to speculate that interruptions of these two pathways fundamentally cause the same mechanistic effect and that the PD-1/PD-L and IL-10 pathways are "linearly" arranged. Along these lines, it may be noteworthy that we obtained a preferential effect of blocking in vivo with anti-PD-L1, compared to anti-PD-L2, MAb, at least at 8 wpi (Fig. 6). There is evidence in several other systems that "reverse" signaling through PD-L can occur upon PD-1/PD-L interactions and that APC stimulation through PD-L1/PD-L2 can result in IL-10 production (6, 38, 71). Similarly, in the LP-BM5 retroviral model used here, ICCS analysis demonstrated that IL-10 production could largely, it not entirely, be ascribed to a $CD11b^+$ $CD11c^-$ CD16/CD32 $(Fc\gamma R)^+$ $F4/80^+$ macrophage/macrophage-like population (Fig. 8 and data not shown). Given that macrophages express PD-L1 and that an expanded population of $CD11b^+$ $CD16/CD32^+$ cells develops in WT B6 mice in an infection-dependent manner (Fig. 1 and 4), such IL-10 production could result from (B-cell) PD-1 occupancy of PD-L1 on these macrophage-like cells. In support of this possibility, in infected PD-1 KO mice, although the expansion of these $CD11b^+$ macrophage-like cells was even greater than that in infected WT B6 mice, no infection-dependent increase in IL-10 production by this subset was observed by either ICCS (Fig. 9) or enzyme-linked immunospot assay analysis. Thus, PD-1 expression was required for the increased IL-10 response, and further studies are required to confirm whether such IL-10 production in WT B6 mice is triggered by binding of specifically PD-L1 to PD-1.

However, other interpretations are possible and clarification of this question awaits additional and challenging experiments required to differentiate these possibilities. These and other issues raised by the results presented here underscore the utility of the LP-BM5 retroviral system for the further study of the effects of blockade of the PD-1/PD-L and IL-10 negative regulatory pathways on antiviral T-cell-mediated immunopathology and provide a cautionary note relative to attempts to enhance protective T-cell immunity in viral diseases where such T cells also cause tissue damage.

ACKNOWLEDGMENTS

We thank Edward Usherwood, Wen Li, On Ho, Melanie Rutkowski, and Tim Carlson for many helpful discussions and technical assistance and Robert Taintor and Wen Li for manuscript assistance. We also thank Jian Zhang for kindly supplying PD-1 KO breeding pairs and Alice Givan and Gary Ward for help with flow cytometry.

This work was supported by National Institutes of Health grants CA50157 and AI059580 (to W.R.G.). Flow cytometry was performed at Dartmouth Medical School in the Herbert C. Englert Cell Analysis Laboratory, which was established by equipment grants from the Fannie E. Rippel Foundation, the NIH Shared Instrument Program, and Dartmouth Medical School and is supported in part by core grant CA23108 from the National Cancer Institute to the Norris Cotton Cancer Center.

REFERENCES

1. **Agata, Y., A. Kawasaki, H. Nishimura, Y. Ishida, T. Tsubata, H. Yaglta, and T. Honjo.** 1996. Expression of the PD-1 antigen on the surface of stimulated mouse T and B lymphocytes. Int. Immunol. **8:**765–772.
2. **Ahonen, C. L., E. M. Manning, L. D. Erickson, B. P. O'Connor, E. F. Lind, S. S. Pullen, M. R. Kehry, and R. J. Noelle.** 2002. The CD40-TRAF6 axis controls affinity maturation and the generation of long-lived plasma cells. Nat. Immunol. **3:**451–452.
3. **Aziz, D. C., Z. Hanna, and P. Jolicoeur.** 1989. Severe immunodeficiency disease induced by a defective murine leukemia virus. Nature **338:**505–508.
4. **Badou, A., Y. Bennasser, M. Moreau, C. Leclerc, M. Benkirane, and E. Bahraoui.** 2000. Tat protein of human immunodeficiency virus type I induces interleukin-10 in human peripheral blood monocytes: implication of protein kinase C-dependent pathway. J. Virol. **74:**10551–10562.
5. **Barber, D. L., E. J. Wherry, D. Masopust, B. Zhu, J. P. Allison, A. H. Sharpe, G. J. Freeman, and R. Ahmed.** 2006. Restoring function in exhausted $CD8^+$ T cells during chronic viral infection. Nature **439:**682–687.
6. **Blocki, F. A., S. Radhakrishnan, V. P. Van Keulen, K. L. Heckman, B. Ciric, C. L. Howe, M. Rodriguez, E. Kwon, and L. R. Pease.** 2006. Induction of a gene expression program in dendritic cells with a cross-linking IgM antibody to the co-stimulatory molecule B7-DC. FASEB J. **20:**2408–2410.
7. **Brooks, D. G., M. J. Trifilo, K. H. Edelmann, L. Teyton, D. B. McGavern, and M. B. A. Oldstone.** 2006. Interleukin-10 determines viral clearance or persistence *in vivo*. Nat. Med. **12:**1301–1309.
8. **Buller, R. M. L., R. A. Yetter, T. N. Fredrickson, and H. C. Morse III.** 1987. Abrogation of resistance to severe mousepox in C57BL/6 mice infected with LP-BM5 murine leukemia viruses. J. Virol. **61:**383–387.
9. **Carreno, B. M., and M. Collins.** 2002. The B7 family of ligands and its receptors: new pathways for costimulation and inhibition of immune responses. Annu. Rev. Immunol. **20:**29–53.
10. **Cerny, A. A., W. Hugin, R. R. Hardy, K. Hayakawa, R. M. Zinkernagel, M. Makino, and H. C. Morse III.** 1990. B cells are required for induction of T cell abnormalities in a murine retrovirus-induced immunodeficiency syndrome. J. Exp. Med. **171:**315–320.
11. **Chattopadhyay, S. K., H. C. Morse III, M. Makino, S. K. Ruscetti, and J. W. Hartley.** 1989. A defective virus is associated with induction of a murine retrovirus-induced immunodeficiency syndrome, MAIDS. Proc. Natl. Acad. Sci. USA **86:**3862–3866.
12. **Cook, W. J., K. A. Green, J. J. Obar, and W. R. Green.** 2003. Quantitative analysis of LP-BM5 murine leukemia retrovirus RNA using real-time RT-PCR. J. Virol. Methods **108:**49–58.
13. **Curiel, T. J., S. Wei, H. Dong, X. Alvarez, P. Cheng, P. Mottram, R. Krzysiek, K. L. Knutson, B. Daniel, M. C. Zimmermann, O. David, M. Burow, A. Gordon, N. Dhurandhar, L. Myers, R. Berggren, A. Hemminki, R. D. Alvarez, D. Emilie, D. T. Curiel, L. Chen, and W. Zou.** 2003. Blockade of B7-H1 improves myeloid dendritic cell-mediated antitumor immunity. Nat. Med. **9:**562–567.
14. **Day, C. L., D. E. Kaufmann, P. Kiepiela, J. A. Brown, E. S. Moodley, S. Reddy, E. W. Mackey, J. D. Miller, A. J. Leslie, C. DePierres, Z. Mncube, J.**

Duraiswamy, B. Zhu, Q. Eichbaum, M. Altfeld, E. J. Wherry, H. M. Coovadia, P. J. R. Goulder, P. Klenerman, R. Ahmed, G. J. Freeman, and B. D. Walker. 2006. PD-1 expression on HIV-specific T cells is associated with T-cell exhaustion and disease progression. Nature **443:**350–354.

15. **Dong, H., G. Zhu, K. Tamada, and L. Chen.** 1999. B7-H1, a third member of the B7 family, co-stimulates T-cell proliferation and interleukin-10 secretion. Nat. Med. **5:**1365–1369.
16. **Dong, H., S. E. Strome, D. R. Salomao, H. Tamura, F. Hirano, D. B. Flies, P. C. Roche, J. Lu, G. Zhu, K. Tamada, V. A. Lennnon, E. Celis, and L. Chen.** 2002. Tumor associated B7-H1 promotes T cell apoptosis: a potential mechanism of immune evasion. Nat. Med. **8:**793–800.
17. **Ejrnaes, M., C. M. Filippi, M. M. Martinic, E. M. Ling, L. M. Togher, S. Crotty, and M. G. Von Herrath.** 2006. Resolution of a chronic viral infection after interleukin-10 receptor blockade. J. Exp. Med. **203:**2461–2472.
18. **Freeman, G. J., A. J. Long, Y. Iwai, K. Bourque, T. Chernova, H. Nishimura, L. J. Fitz, N. Malenkovich, T. Okazaki, M. C. Byrne, H. F. Horton, L. Fouser, L. Carter, V. Ling, M. R. Bowman, B. M. Carreno, M. Collins, C. R. Wood, and T. Honjo.** 2000. Engagement of the PD-1 immunoinhibitory receptor by a novel B7 family member leads to negative regulation of lymphocyte activation. J. Exp. Med. **192:**1027–1034.
19. **Freeman, G. J., E. J. Wherry, R. Ahmed, and A. H. Sharpe.** 2006. Reinvigorating exhausted HIV-specific T cells via PD-1-PD-1 ligand blockade. J. Exp. Med. **203:**2223–2227.
20. **Green, K. A., C. L. Ahonen, W. J. Cook, and W. R. Green.** 2004. CD40-Associated TRAF 6 signaling is required for disease induction in a retrovirus-induced murine immunodeficiency. J. Virol. **78:**6055–6060.
21. **Green, K. A., K. M. Crassi, J. D. Laman, A. Schoneveld, R. R. Strawbridge, T. M. Foy, R. J. Noelle, and W. R. Green.** 1996. Antibody to the ligand for CD40 (gp39) inhibits murine AIDS-associated splenomegaly, hypergammaglobulinemia, and immunodeficiency in disease-susceptible C57BL/6 mice. J. Virol. **70:**2569–2575.
22. **Green, K. A., R. J. Noelle, and W. R. Green.** 1998. Evidence for a continued requirement for CD40/CD40 ligand (CD154) interactions in the progression of LP-BM5 retrovirus-induced murine AIDS. Virology **241:**260–268.
23. **Green, K. A., R. J. Noelle, B. G. Durell, and W. R. Green.** 2001. Characterization of the CD154-positive and CD40-positive cellular subsets required for pathogenesis in retrovirus-induced murine immunodeficiency. J. Virol. **75:**3581–3589.
24. **Green, K. A., W. J. Cook, A. H. Sharp, and W. R. Green.** 2002. The CD154/CD40 interaction required for retrovirus-induced murine immunodeficiency syndrome is not mediated by upregulation of the CD80/CD86 costimulatory molecules. J. Virol. **76:**13106–13110.
25. **Greenwald, R. J., G. J. Freeman, and A. H. Sharpe.** 2005. The B7 family revisited. Annu. Rev. Immunol. **23:**515–548.
26. **Hartley, J. W., T. N. Fredrickson, R. A. Yetter, M. Makino, and H. C. Morse III.** 1989. Retrovirus-induced murine acquired immunodeficiency syndrome: natural history of infection and differing susceptibility of inbred mouse strains. J. Virol. **63:**1223–1230.
27. **Ho, O., and W. R. Green.** 2006. Cytolytic $CD8^+$ T cells directed against a cryptic epitope derived from a retroviral alternative reading frame confer disease protection. J. Immunol. **176:**2470–2475.
28. **Huang, M., C. Simard, and P. Jolicoeur.** 1989. Immunodeficiency and clonal growth of target cells induced by helper-free defective retrovirus. Science **246:**1614–1617.
29. **Ishida, M., Y. Iwai, Y. Tanaka, T. Okazaki, G. J. Freeman, N. Minato, and T. Honjo.** 2002. Differential expression of PD-L1 and PD-L2, ligands for an inhibitory receptor PD-1, in the cells of lymphohematopoietic tissues. Immunol. Lett. **84:**57–62.
30. **Ishida, Y., Y. Agata, K. Shibahara, and T. Honjo.** 1992. Induced expression of PD-1, a novel member of the immunoglobulin gene superfamily, upon programmed cell death. EMBO J. **11:**3887–3895.
31. **Isogawa, M., Y. Furuichi, and F. V. Chisari.** 2005. Oscillating $CD8^+$ T cell effectors functions after antigen recognition in the liver. Immunity **23:**53–63.
32. **Jones, K. W., and C. J. Hackett.** 1996. Activated T hybridomas induce upregulation of B7-1 on bystander B lymphoma cells by a contact-dependent interaction utilizing CD40 ligand. Cell. Immunol. **174:**42–53.
33. **Klinken, S. P., T. N. Fredrickson, J. W. Hartley, R. A. Yetter, and H. C. Morse III.** 1988. Evolution of B cell lineage lymphomas in mice with a retrovirus-induced immunodeficiency syndrome, MAIDS. J. Immunol. **140:**1123–1131.
34. **Klinman, D. M., and H. C. Morse III.** 1989. Characteristics of B cell proliferation and activation in murine AIDS. J. Immunol. **142:**1144–1149.
35. **Knoetig, S. M., T. A. Torrey, Z. Naghashfar, T. McCarty, and H. C. Morse III.** 2002. CD19 signaling pathways play a major role for murine AIDS induction and progression. J. Immunol. **169:**5607–56614.
36. **Kühn, R., D. J. Lohler, D. Rennick, K. Rajewsky, and W. Muller.** 1993. Interleukin-10-deficient mice develop chronic enterocolitis. Cell **75:**263–274.
37. **Kuhné, M. R., M. Robbins, J. E. Hambor, M. F. Mackey, Y. Kosaka, T. Nishimura, J. P. Gigley, R. J. Noelle, and D. M. Calderhead.** 1997. Assembly and regulation of the CD40 receptor complex in human B cells. J. Exp. Med. **186:**337–342.
38. **Kuipers, H., F. Muskens, M. Willart, D. Hijdra, F. B. J. van Assema, A. J. Coyle, H. C. Hoogsteden, and B. N. Lambrecht.** 2006. Contribution of the PD-1 ligands/PD-1 signaling pathway to dendritic cell-mediated $CD4^+$ T cell activation. Eur. J. Immunol. **36:**2472–2482.
39. **Latchman, Y., C. R. Wood, T. Chernova, D. Chaudhary, M. Borde, I. Chernova, Y. Iwai, A. J. Long, J. A. Brown, R. Nunes, E. A. Greenfield, K. Bourque, V. A. Boussiotis, L. L. Carter, B. M. Carreno, N. Malenkovich, H. Nishimura, T. Okazaki, T. Honjo, A. H. Sharpe, and G. J. Freeman.** 2001. PD-L2 is a second ligand for PD-1 and inhibits T cell activation. Nat. Immunol. **2:**261–268.
40. **Legrand, E., R. Daculsi, and J. F. Duplan.** 1981. Characteristics of the cell populations involved in extrathymic lymphosarcoma induced in C57BL/6 mice by RadLV-RS. Leuk. Res. **5:**223–233.
41. **Li, W., and W. R. Green.** 2007. Murine AIDS requires CD154/CD40L expression by the $CD4^+$ T cells that mediate retrovirus-induced disease: is $CD4^+$ T cell receptor ligation needed? Virology **360:**58–71.
42. **Li, W., and W. R. Green.** 2006. The role of $CD4^+$ T cells in the pathogenesis of murine AIDS. J. Virol. **80:**5777–5789.
43. **Macchia, D., P. Parronchi, M. P. Piccinni, C. Simonelli, M. Mazzetti, A. Ravina, D. Milo, E. Maggi, and S. Romagnani.** 1991. *In vitro* infection with HIV enables human $CD4^+$ T cell clones to induce noncognate contact-dependent polyclonal B cell activation. J. Immunol. **146:**3413–3418.
44. **Mayrand, S. M., D. A. Schwarz, and W. R. Green.** 1998. An alternative translational reading frame encodes an immunodominant retroviral CTL determinant expressed by an immunodeficiency causing retrovirus. J. Immunol. **160:**39–50.
45. **Mayrand, S. M., P. A. Healy, B. E. Torbett, and W. R. Green.** 2000. Anti-*gag* cytolytic T lymphocytes specific for an alternative translational reading frame-derived epitope and resistance versus susceptibility to retrovirus-induced murine AIDS in F_1 mice. Virology **272:**438–449.
46. **Morse, H. C., III, R. A. Yetter, C. S. Via, R. R. Hardy, A. Cerny, K. Hayakawa, A. W. Hugin, M. W. Miller, K. L. Homes, and G. M. Shearer.** 1989. Functional and phenotypic alterations in T cell subsets during the course of MAIDS, a murine retrovirus-induced immunodeficiency syndrome. J. Immunol. **143:**844–850.
47. **Mosier, D. E., R. A. Yetter, and H. C. Morse III.** 1985. Retroviral induction of acute lymphoproliferative disease and profound immunosuppression in adult C57BL/6 mice. J. Exp. Med. **161:**766–784.
48. **Mosier, D. E., R. A. Yetter, and H. C. Morse III.** 1987. Functional T lymphocytes are required for a murine retrovirus-induced immunodeficiency disease (MAIDS). J. Exp. Med. **165:**1732–1742.
49. **Müller, F., P. Aukrust, I. Nordoy, and S. S. Froland.** 1998. Possible role of interleukin-10 (IL-10) and CD40 ligand expression in the pathogenesis of hypergammaglobulinemia in human immunodeficiency virus infection: modulation of IL-10 and Ig production after intravenous Ig infusion. Blood **92:**3721–3729.
50. **Nishimura, H., N. Minato, T. Nakano, and T. Honjo.** 1998. Immunological studies on PD-1-deficient mice: implication of PD-1 as a negative regulator for B cell responses. Int. Immunol. **10:**1563–1572.
51. **Okazaki, T., and T. Honjo.** 2006. The PD-1–PD-L pathway in immunological tolerance. Trends Immunol. **27:**195–201.
52. **Okazaki, T., Y. Iwai, and T. Honjo.** 2002. New regulatory co-receptors: inducible costimulator and PD-1. Curr. Opin. Immunol. **14:**779–782.
53. **Okazaki, T., A. Maeda, H. Nishimura, T. Kurosaki, and T. Honjo.** 2001. PD-1 immunoreceptor inhibits B cell receptor-mediated signaling by recruiting src homology 2-domain-containing tyrosine phosphatase 2 to phosphotyrosine. Proc. Natl. Acad. Sci. USA **98:**13866–13871.
54. **Pattengale, P. K., C. R. Taylor, P. Twomey, S. Hill, J. Jonasson, T. Beardsley, and M. Haas.** 1982. Immunopathology of B cell lymphomas induced in C57BL/6 mice by dualtropic murine leukemia virus (MuLV). Am. J. Pathol. **107:**362–377.
55. **Petrovas, C., J. P. Casazza, J. M. Brenchley, D. A. Price, E. Gostick, W. C. Adams, M. L. Precopio, T. Schacker, M. Roederer, D. C. Douek, and R. A. Koup.** 2006. PD-1 is a regulator of virus-specific $CD8^+$ T cell survival in HIV infection. J. Exp. Med. **203:**2281–2292.
56. **Pullen, S. S., H. G. Miller, D. S. Everdeen, T. T. Dang, J. J. Crute, and M. R. Kehry.** 1998. CD40-tumor necrosis factor receptor-associated factor (TRAF) interactions: regulation of CD40 signaling through multiple TRAF binding sites and TRAF hetero-oligomerization. Biochemistry **37:**11836–11845.
57. **Pullen, S. S., T. T. Dang, J. J. Crute, and M. R. Kehry.** 1999. CD40 signaling through tumor necrosis factor receptor-associated factors (TRAFs). Binding specificity and activation of downstream pathways by distinct TRAFs. J. Biol. Chem. **274:**14246–14254.
58. **Ranheim, E. A., and T. J. Kipps.** 1995. Tumor necrosis factor facilitates induction of CD80 (B7-1) and CD54 on human B cells by activated T cells: complex regulation by IL-4, IL-10 and CD40L. Cell. Immunol. **161:**226–235.
59. **Ranheim, E. A., and T. J. Kipps.** 1993. Activated T cells induce expression of B7/BB1 on normal or leukemic B cells through a CD40-dependent signal. J. Exp. Med. **177:**925–935.
60. **Rowe, W. P., W. E. Pugh, and J. W. Hartley.** 1970. Plaque assay techniques for murine leukemia viruses. Virology **42:**1136.
61. **Roy, M., A. Aruffo, J. Ledbetter, P. Linsley, M. Kehry, and R. Noelle.** 1995. Studies on the interdependence of gp39 and B7 expression and function during antigen-specific immune responses. Eur. J. Immunol. **25:**596–603.

62. **Saunders, P. A., V. R. Hendrycks, W. A. Lindinsky, and M. L. Woods.** 2005. PD-L2:PD-1 involvement in T cell proliferation, cytokine production, and integrin-mediated adhesion. Eur. J. Immunol. **35:**3561–3569.
63. **Schwarz, D. A., and W. R. Green.** 1994. CTL responses to the *gag* polyprotein encoded by the murine AIDS defective retrovirus are strain dependent. J. Immunol. **153:**436–441.
64. **Selenko-Gebauer, N., O. Majdic, A. Szekeres, G. Höfler, E. Guthann, U. Korthäuer, G. Zlabinger, P. Steinberger, W. F. Pickl, H. Stockinger, W. Knapp, and J. Stöckl.** 2003. B7-H1 (programmed death-1 ligand) on dendritic cells is involved in the induction and maintenance of T cell anergy. J. Immunol. **170:**3637–3644.
65. **Sharpe, A. H., E. J. Wherry, R. Ahmed, and G. J. Freeman.** 2007. The function of programmed cell death 1 and its ligands in regulating autoimmunity and infection. Nat. Immunol. **8:**239–245.
66. **Simard, C., S. J. Klein, T. Mak, and P. Jolicoeur.** 1997. Studies of the susceptibility of nude, CD4 knockout, and SCID mutant mice to the disease induced by the murine AIDS defective virus. J. Virol. **71:**3013–3022.
67. **Strome, S. E., H. Dong, H. Tamura, S. G. Voss, D. B. Flies, K. Tamada, D. Salomao, J. Cheville, F. Hirano, W. Lin, J. L. Kasperbauer, K. V. Ballman, and L. Chen.** 2003. B7-H1 blockade augments adoptive T-cell immunotherapy for squamous cell carcinoma. Cancer Res. **63:**6501–6505.
68. **Tamura, H., H. Dong, G. Zhu, G. L. Sica, D. B. Flies, K. Tamada, and L. Chen.** 2001. B7-H1 costimulation preferentially enhances CD28-independent T-helper cell function. Blood **97:**1809–1816.
69. **Trautmann, L., L. Janbazian, N. Chomont, E. A. Said, S. Gimmig, B. Bessette, M. Boulassel, E. Delwart, H. Sepulveda, R. S. Balderas, J. Routy, E. K. Haddad, and R. Sekaly.** 2006. Upregulation of PD-1 expression on HIV-specific $CD8^+$ T cells leads to reversible immune dysfunction. Nat. Med. **12:**1198–1202.
70. **Urbani, S., B. Amadei, D. Tola, M. Massari, S. Schivazappa, G. Missale, and C. Ferrari.** 2006. PD-1 expression in acute hepatitis C virus (HCV) infection is associated with HCV-specific CD8 exhaustion. J. Virol. **80:**11398–11403.
71. **Van Keulen, V. P., B. Ciric, S. Radhakrishnan, K. L. Heckman, Y. Mitsunaga, K. Iijima, H. Kita, M. Rodriquez, and L. R. Pease.** 2006. Immunomodulation using the recombinant monoclonal human B7-DC cross-linking antibody rHIgM12. Clin. Exp. Immunol. **143:**314–321.
72. **Yamazaki, T., A. Hisaya, H. Iwai, H. Matsuda, M. Aoki, Y. Tanno, T. Shin, H. Tsuchiya, D. Pardoll, K. Okumura, M. Azuma, and H. Yagita.** 2002. Expression of programmed death 1 ligands by murine T cells and APC. J. Immunol. **169:**5538–5545.
73. **Yetter, R. A., R. M. L. Buller, J. S. Lee, K. L. Elkins, D. E. Mosier, T. N. Fredrickson, and H. C. Morse III.** 1988. $CD4^+$ T cells are required for development of a murine retrovirus-induced immunodeficiency syndrome (MAIDS). J. Exp. Med. **168:**623–635.
74. **Yu, P., R. A. Morawetz, S. Chattopadhyay, M. Makino, T. Kishimoto, and H. Kikutani.** 1999. CD40-deficient mice infected with the defective murine leukemia virus LP-BM5def do not develop murine AIDS but produce IgE and IgG1 in vivo. Eur. J. Immunol. **29:**615–625.